

Seismic attenuation and rock property analysis in a heavy oilfield: Ross Lake, Saskatchewan

Zimin Zhang and Robert R. Stewart

ABSTRACT

We analyze the relationship between seismic data attenuation and rock properties in well 11-25-13-17W3 from the Ross Lake heavy oilfield, Saskatchewan. Well log analysis indicates that the main lithologies in this well are shale and shaly sandstone. Interval Q values for the P wave and shear wave were estimated by applying the spectral ratio method on VSP data (which used both vertical and horizontal vibrators). The Q values are most reliable from 400m to 1050m for the P wave and from 225m to 1050m for the shear wave. The Q values correlate interestingly with petrophysical variables. Q_p values increase with P- and S-velocities and decrease with V_p/V_s and porosity. Shaly sandstone shows more attenuation than pure shale and sandstone. The crossplot between Q_p and clay-bound water indicates more attenuation in shaly sandstone possibly caused by the interaction between mobile water and clay-bound water. Q values for S-waves also display a similar relationship. Velocity dispersion was observed between VSP-derived velocities and sonic velocities. Sonic log velocities are 3.4% higher than VSP velocities in average for P wave, and 4.8% higher averagely for shear wave.

INTRODUCTION

Attenuation is one of the basic seismic attributes of waves propagating in the earth. Understanding the causes of attenuation and the relationship between attenuation of seismic data and rock properties is important in the acquisition, processing and interpretation of seismic data. A number of authors have examined the relationship between attenuation and rock properties for seismic data interpretation and reservoir characterization (eg., Klimentos and McCann, 1990; Koesoemadinata and McMechan, 2001). In this study, well log data and VSP data will be used for the analysis of the relationship between rock properties and attenuation. Based on this study, attenuation characteristics of seismic data are expected to provide helpful information for seismic interpretation and reservoir characterization.

The well selected for this study is the well 11-25-13-17W3 from Ross Lake, Saskatchewan. The lithologies of studied interval are mainly shale and shaly sandstone. The producing reservoir in this well is a Cretaceous-age channel sand in the Cantuar formation of the Mannville Group. The produced oil is heavy, about 13° API (from Xu and Stewart, 2003). A multi-offset VSP survey was conducted in June 2003. The zero-offset VSP survey used both vertical and horizontal vibrators as sources, which are favorable for estimation P- and S-wave attenuation. Density and neutron porosity, dipole sonic and resistivity logs were also available in this well.

WELL LOG ANALYSIS

Figure 1 displays well log curves with formation tops of well 11-25-13-17W3 from Ross Lake heavy oilfield. There are two clean sand intervals with good permeability at 1148m-1160m and 1164m-1180m respectively (Figure 2), which are interpreted to be sand channels in the Cantuar formation. There was about 12m of oil pay of the upper sand, while the lower sand was wet. Between the upper and lower sand, there is a tight formation with small porosity, about 7%. Clay content in the rock was estimated from the gamma-ray curve by linear scaling between its minimum and maximum values. The total porosity was calculated from the average of density-porosity and neutron-porosity logs. Effective porosity was estimated from the average of the shale-corrected density-porosity and neutron-porosity. Water saturation in this well was calculated from the resistivity curve based on Simondoux model. The results are plotted as Figure 3. The porosity of the channel sand is quite high, about 30%. PE log was unavailable in this well. According to neutron-density porosity difference and regional geology in southwest Saskatchewan, the lithologies in this well are mostly shale, shaly sandstone and sandstone.

For the shallow part (above Milk River Formation) in this well, the rocks seem to be very shaly, the shale content is more than 50%, while the calculated porosities are quite high. The total porosity is approximately 40%. The effective porosity is about 20%. To investigate the reason for such high porosity, crossplot between total porosity and P-wave velocity was created (Figure 4). From the characteristics of well log curve, the P-wave velocity and total porosity were separated into three parts: depth 198m to 617m (the data in blue), depth 617m to 781m (the data in red), and 781m to the bottom of the well (the data in green). These three groups distribute differently in V_p and total porosity crossplot. According to the model described in the paper by Mukerji and Mavko (2006), it perhaps indicates diagenesis differences of these three depth ranges. The data of the shallow part are mostly around suspension line and display poor cementation. The compaction and diagenesis of the rock are poor at shallow part of this well, much water were preserved in the rock. The rock below Milk River Formation displays much better diagenesis. Clean sand tends to be within a narrow region and relatively far from suspension line. Shaly sand and sandy shale generally locate on the left side of clean sand.

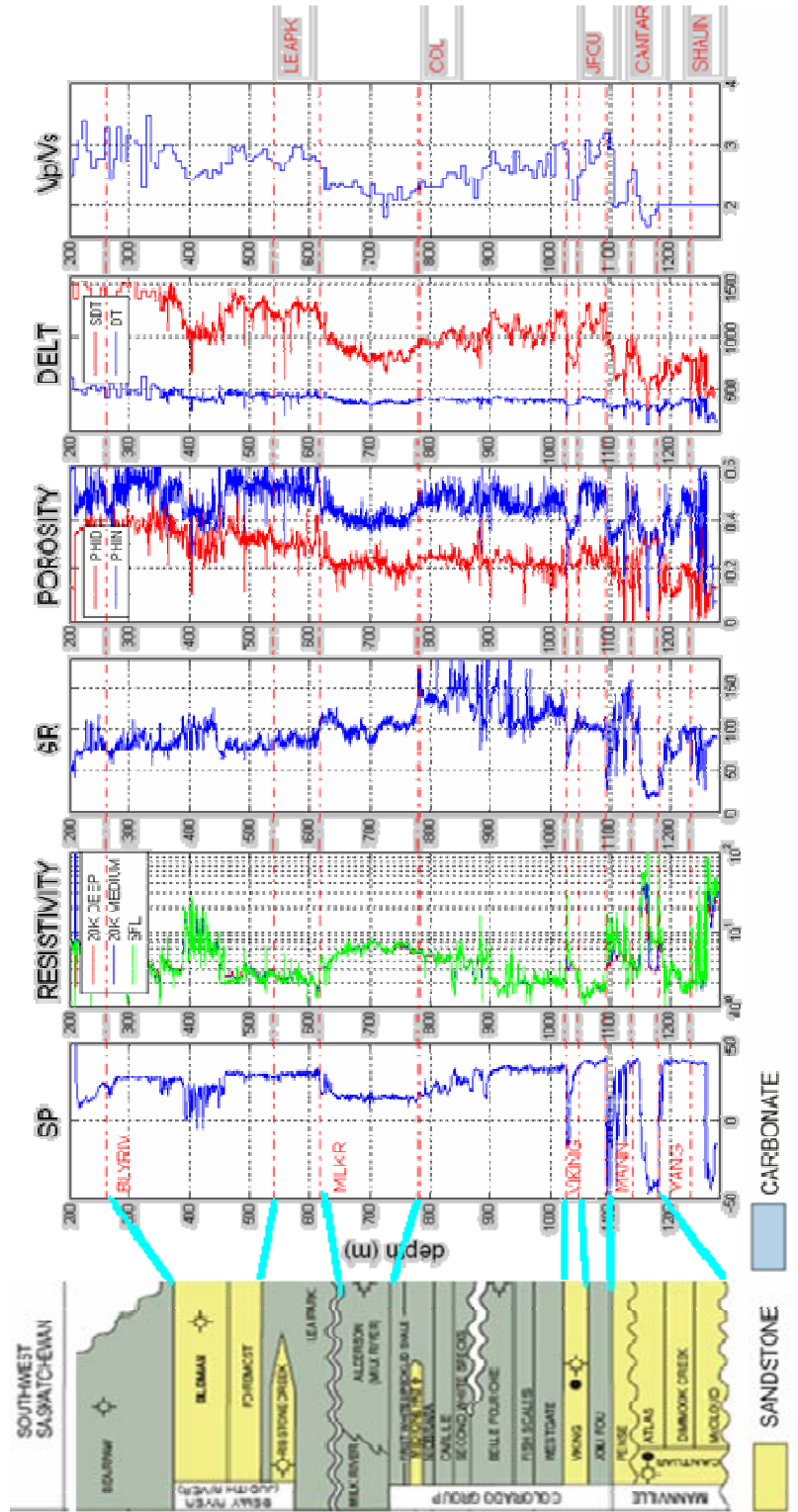


FIG. 1. Regional table of formations and well log curves for the Well 11-25-13-17W3 (with formation tops, the lines represent correlation between regional table of formations and formation tops in this well). From left to right - regional table of formations for southwest Saskatchewan; spontaneous potential (SP); resistivity (deep measurement in blue and shallow tools in green); gamma-ray (GR); density porosity (red, sandstone-scale) and neutron porosity (blue, sandstone-scale); slowness (DELT, shear wave in blue, and P wave in red); and Vp/Vs.

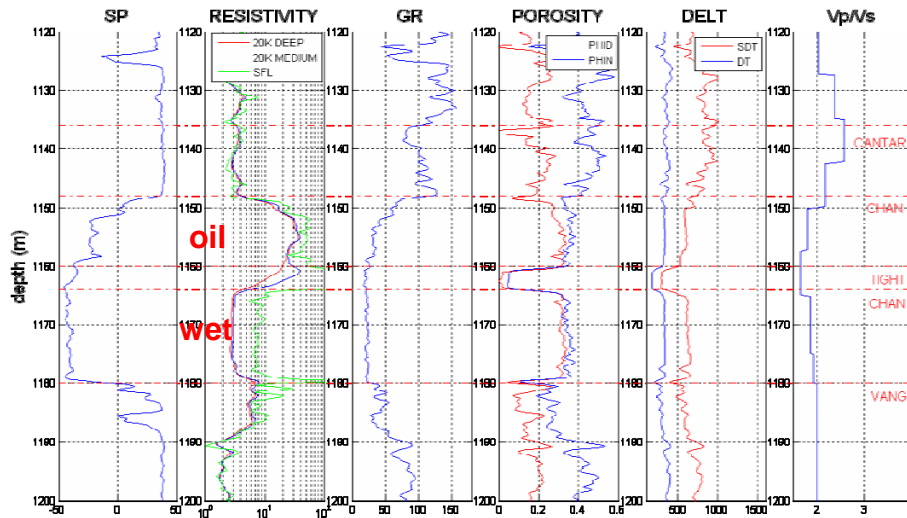


FIG. 2. Well log curves from Figure 1, focusing on the channel sand part of the well.

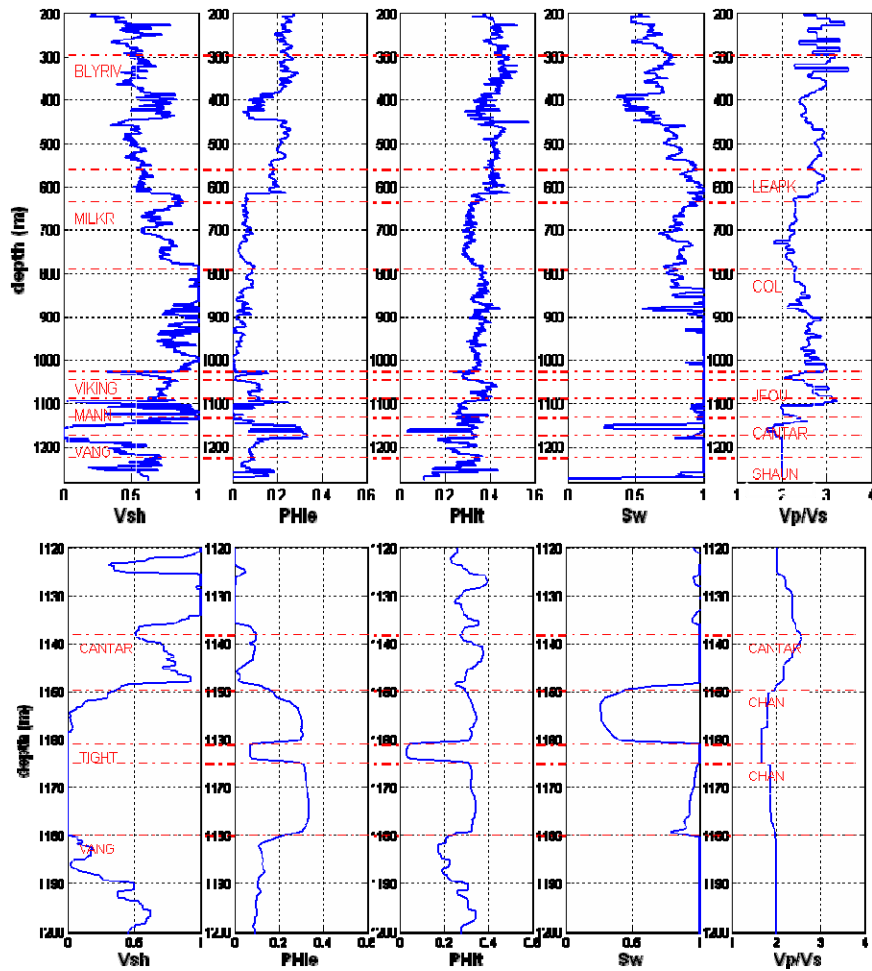


FIG. 3. Top, rock properties from well log data, from left to right: shale volume; effective porosity; water saturation; and Vp/Vs. Bottom, rock properties from the top, focusing on the channel sand part of the well.

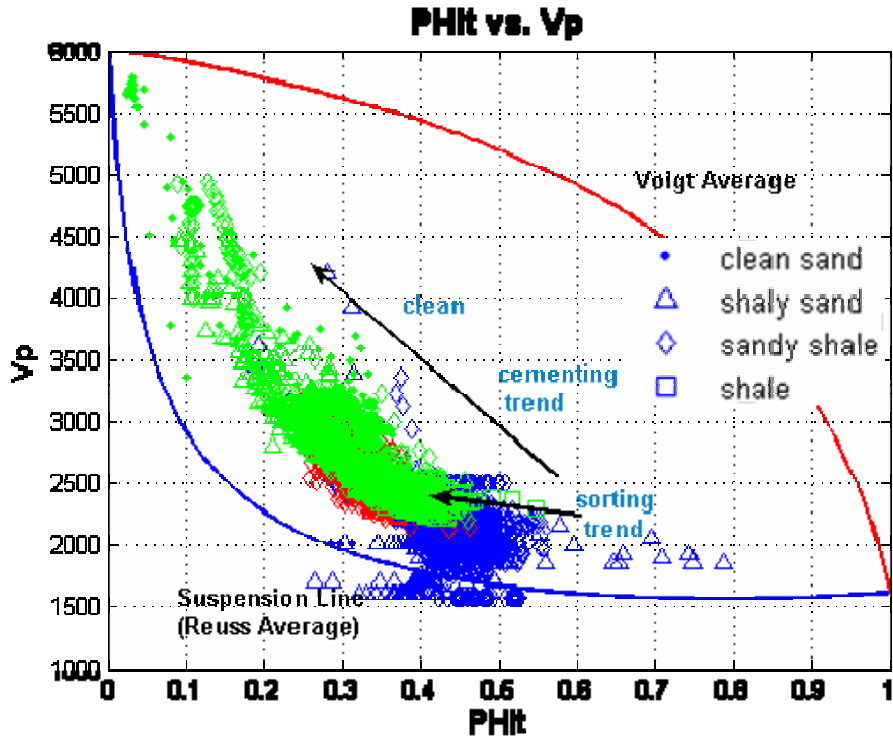


FIG. 4. Crossplot between total porosity and Vp. Blue: 198-617m (above Milk River); red: 617-781m (Milk River-Colorado Group); green: 781-1276m (Colorado group and below).

ATTENUATION ESTIMATION

The spectral ratio method (Hauge, 1981; Toksöz and Johnson, 1981) is widely used for Q value estimation from VSP data. For downgoing waves $g_1(t)$ and $g_2(t)$ recorded at depths Z_1 and Z_2

$$G_2(f) = kG_1(f)e^{-Af} \tag{1}$$

$$A = \frac{-|\omega|}{2Q} (t_2 - t_1) \tag{2}$$

where $G(f)$ is the amplitude spectrum, f is frequency and k is a frequency independent factor that accounts for amplitude effects such as spherical divergence, variations in recording gain, and changes in source and receiver coupling. The exponent, A , is the cumulative seismic wave attenuation between depths Z_1 and Z_2 , and it is also assumed to be independent of frequency. This equation can be rewritten as

$$\ln \left[\frac{G_2(f)}{G_1(f)} \right] = -Af + \ln(K) \quad (3)$$

The left side of this equation is the spectral ratio of the two VSP responses recorded at Z_1 and Z_2 . The cumulative attenuation value is determined by the slope of the best straight line fit to this spectral ratio trend. Thus the average Q value Q_{ave} between depths Z_1 and Z_2 can be calculated from cumulative attenuation.

Bale, et al. (2002) provided a formula to calculate interval Q value from Q_{ave} for a layered medium

$$\frac{T(n)}{Q_{ave}(n)} = \frac{T(n+1)}{Q_{ave}(n+1)} - \frac{T(n+1) - T(n)}{Q_{ave}(n+1)}, \quad n=1,2, \dots, N-1 \quad (4)$$

To estimate Q values for the P wave and S wave, vertical vibrator and horizontal vibrator zero-offset (offset 53.64m) VSP records were used. To redistribute the whole P first arrival energy of vertical vibrator VSP data to a single component, hodogram analysis was used to determine the polarization of different wave modes, and then data rotation was applied. A similar operation was also undertaken for horizontal vibrator VSP data, thus the shear first arrival energy was redistributed to transverse component. Figure 5 displays the vertical component data and the transverse component data from vertical vibrator and horizontal vibrator VSP records respectively. Different attenuation characters for P wave and shear wave can be found. Down-going P- and shear-waves (Figure 6) were then extracted using F-K filter from these two data respectively. It is clear that shear wave was attenuated much more severely than P wave. Then, the amplitude spectra for all the levels were calculated using a 500ms window. Considering the signal-to-noise ratio, frequency bands from 20Hz to 120 Hz for P wave and 20Hz to 40 Hz for shear wave were chosen to build the cumulative attenuation curves for Q value estimation (Figure 7). To avoid unreasonable Q values, the cumulative attenuation curves were smoothed using a 7-point smoothing window before calculating average Q values from the surface to each depth. Using formula (4) attenuation-depth structures for P wave and shear wave were determined from smoothed average Q values using a 21-point window (the right curves of Figure 7). The Q_p values are from 20 to 120, and Q_s values range from 10 to 80. All of them are in reasonable value range. They are also comparable to average Q values by Haase and Stewart (2004), which are 67 for the P-wave and 23 for the shear-wave over an interval of 200m to 1200m.

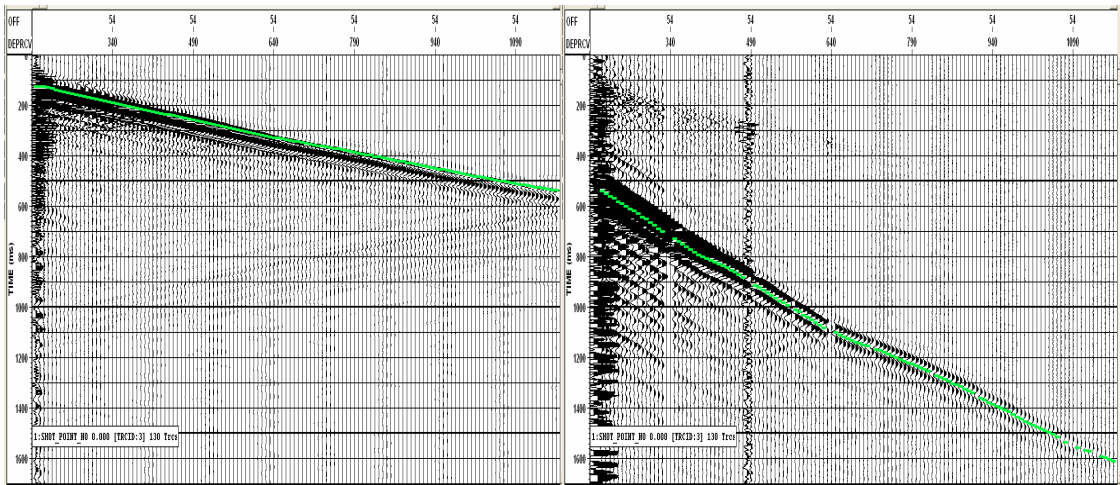


FIG. 5. Vertical component of vertical vibrator VSP data (left) and transverse component of horizontal vibrator VSP data (right).

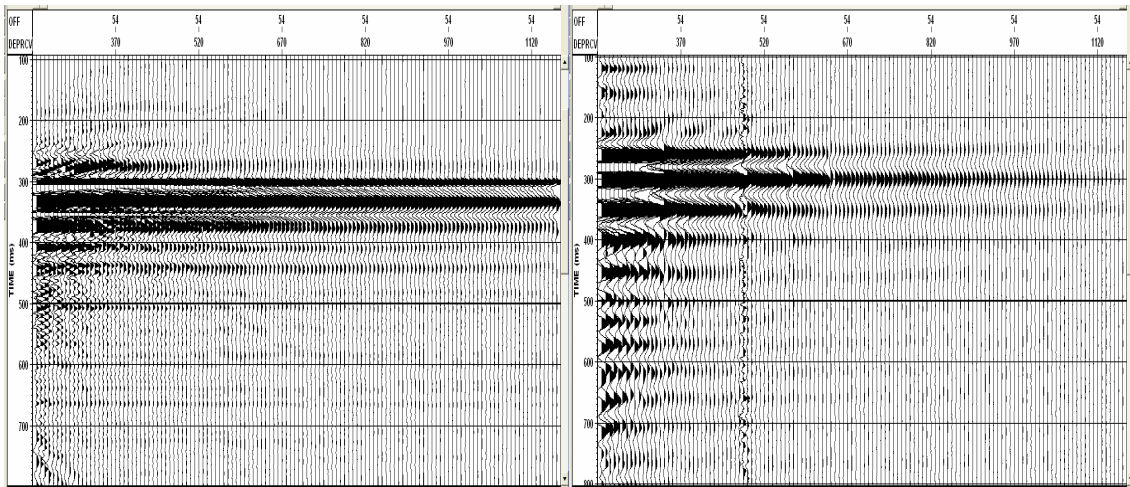


FIG. 6. Flattened down-going P wave (left) and shear wave (right).

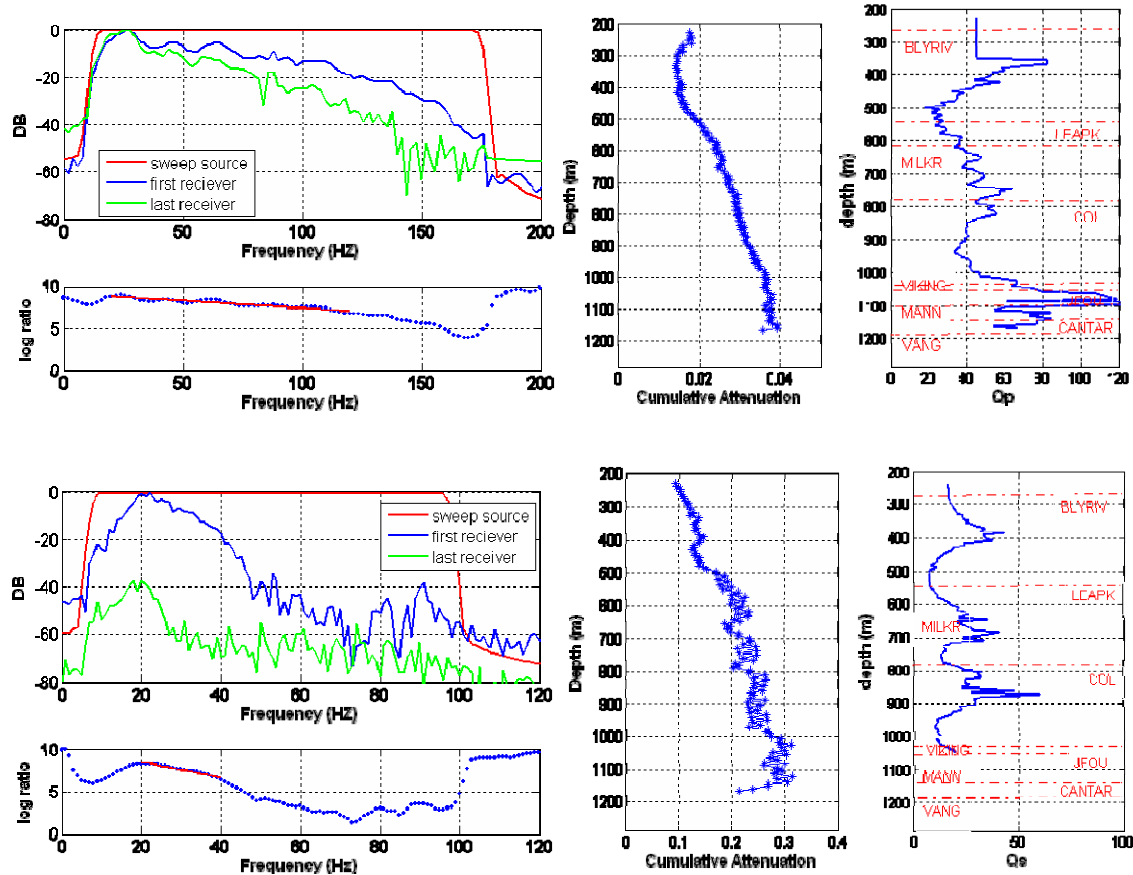


FIG. 7. Top, from left to right - amplitude spectrum and spectral ratio (sweep source in red, the first depth level in blue and the bottom receiver in green); cumulative attenuation calculated from the spectral ratio method; and estimated interval Q values of P wave. The bottom plots are for the shear wave. Using the sweep source and the first depth level, the average attenuations from the surface to the first receiver were 23.3 (Qp), 20 (Qs) for P wave and shear wave respectively.

Q VALUES AND ROCK PROPERTIES

From the cumulative attenuation curve in Figure 7, it can be seen that the values gradually increased with depth from 400m to 1050m. Thus Q values for P wave are considered reliable for this interval. For shear waves, since the frequency bandwidth for Q estimation was narrow, the accumulative attenuation at each depth level was a little dispersed. And a decreasing accumulative attenuation was found over some local parts and the bottom part of the well, which means the interval Q value will be negative (not physically reasonable). Therefore, the following analysis will be focus on the depth intervals with reliable Q values.

Figure 8 displays Q values for P-wave and shear-wave and rock properties from well log analysis. Some correlations between Q values and rock properties can be seen from these curves. Generally high attenuation corresponds to low velocity, high porosity and high Vp/Vs ratio, and vice versa.

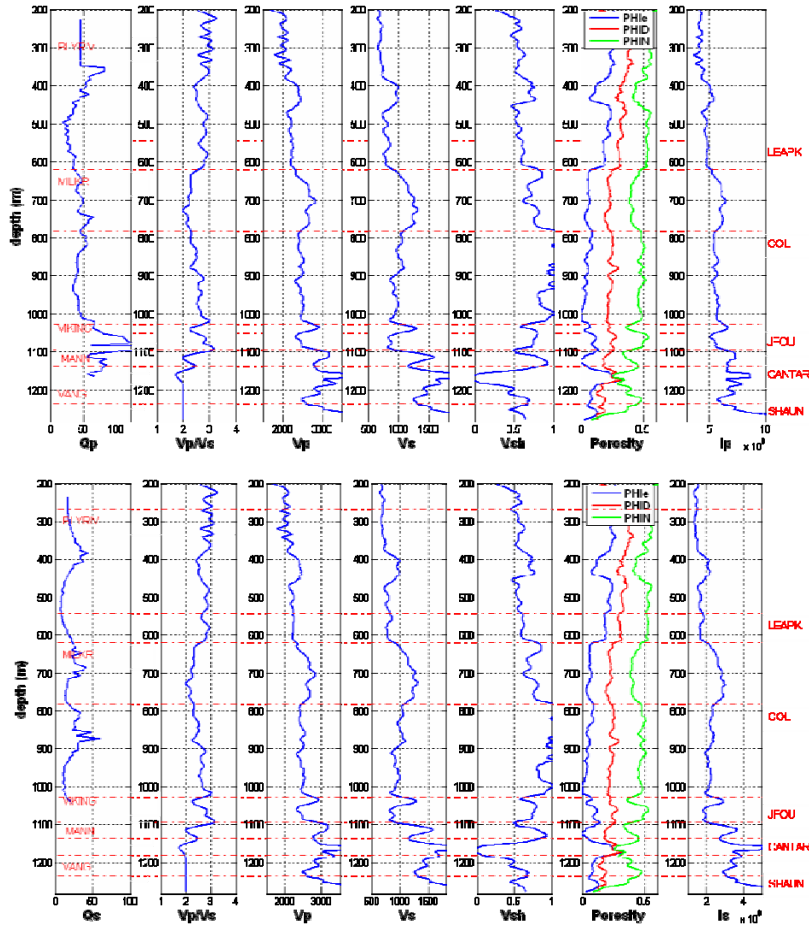


FIG. 8. Top, from left to right – Q_p , V_p/V_s , V_p , V_s , shale volume, porosity (effective porosity in blue, density porosity in red and neutron density in green), and P-wave impedance. The bottom plots are for the S wave (the right frame is shear-wave impedance). Well log data were smoothed using a 15m window.

Q vs. velocity

Figure 9 displays P- and S-wave velocities from well log and VSP data. VSP-derived velocities and well log measured velocities display the same variations with depth, while velocities from well log measurement are generally higher than that from VSP. The velocity differences were calculated by subtracting VSP-measured velocities from sonic velocities and then divided by sonic velocities for P- and shear wave respectively (the second and fourth frame in Figure 9). Sonic log velocities are 3.4% higher than VSP velocities in average for P wave, and 4.8% higher averagely for shear wave. The top part of Figure 10 shows Q_p , P- and shear-wave velocities from well log and VSP data. Q_p values present the similar variation trend with P- and shear velocity. From the crossplot between Q_p values and P- and shear-velocities (bottom part of Figure 10), it can be seen that Q_p values increase linearly with P and shear velocities. A similar variation is also observed for Q_s values and velocities (Figure 11), although the correlation is not as strong as with the Q_p values.

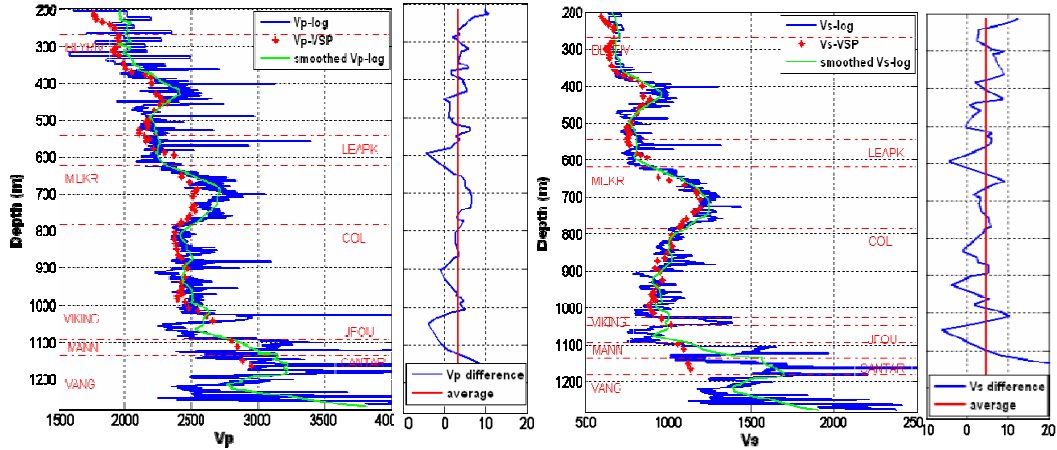


FIG. 9. From left to right: Vp (log P-velocity in blue, smoothed log P-velocity in green, VSP P-velocity in red); log P- and VSP P-velocity difference in percentage (the red line is average difference, 3.4%); Vs (log S-velocity in blue, smoothed log S-velocity in green, VSP S-velocity in red), log S- and VSP S-velocity difference in percentage (the red line is average difference, 4.8%).

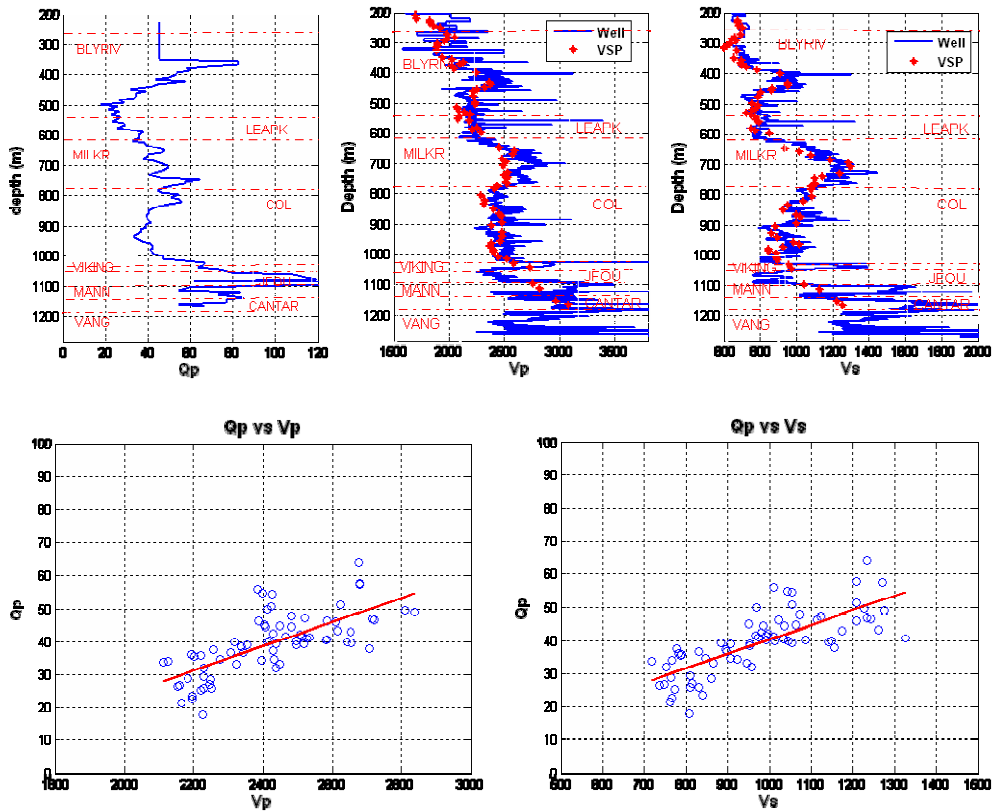


FIG.10. Top - Qp from zero-offset VSP data (left), P velocity from well log (blue line of right) and P velocity from VSP data (red star of right). Bottom - crossplot between Qp and P velocity (left) and Qp vs. shear velocity (right).

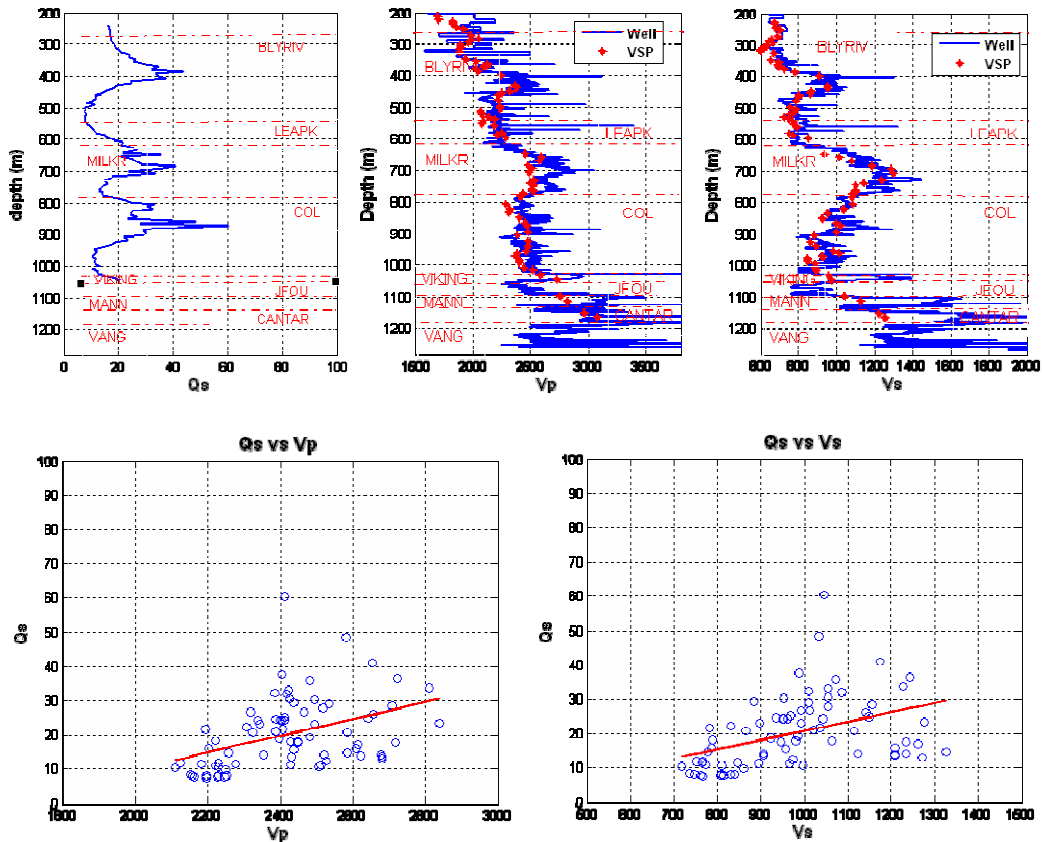


FIG. 11. Top - Q_s from zero-offset VSP data (left), shear velocity from well log (blue line of right) and shear velocity from VSP data (red star of right). Bottom - crossplot between Q_s and P velocity (left) and Q_s vs. shear velocity (right).

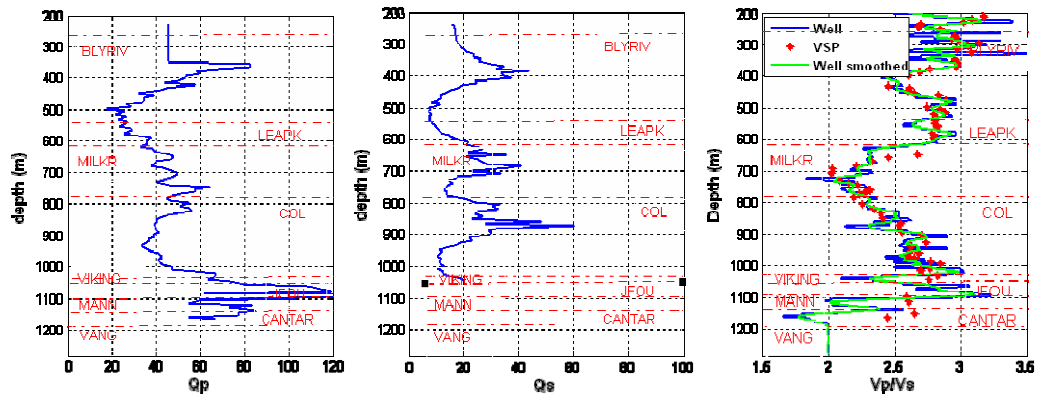


FIG. 12. Interval Q_p value from zero-offset VSP data (left), V_p/V_s value from well log (blue line of right) and V_p/V_s from VSP data (red star of right). The green line is V_p/V_s from well log data smoothed using 10m window.

Q vs. V_p/V_s

Figure 12 displays the Q values of P- and shear-wave and V_p/V_s from well log and VSP data. VSP-derived V_p/V_s correlates with log-measured V_p/V_s quite well. Interval Q_p displays nice correlation with V_p/V_s value. Q_p values generally decrease with

increasing V_p/V_s (Figure 13). Q_s shows the similar trends, but it is not as distinct as that of Q_p (Figure 13).

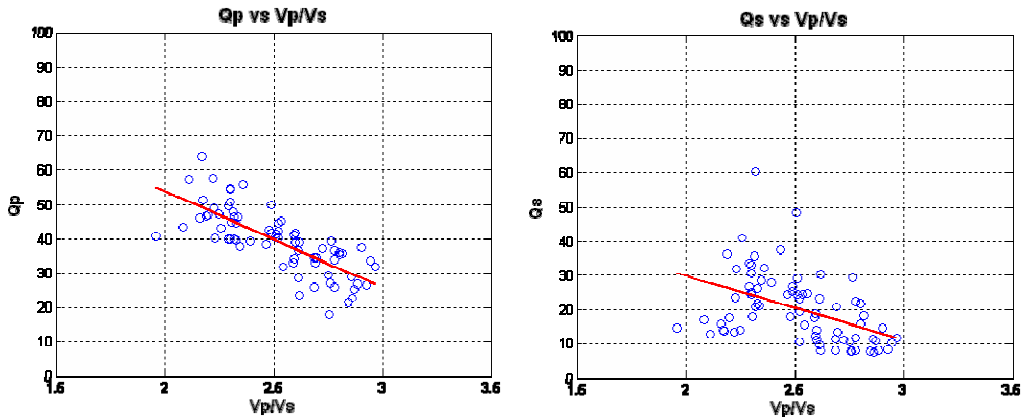


FIG. 13. Crossplot between Q_p and V_p/V_s (left) and Q_s vs. V_p/V_s (right).

Q vs. porosity

Crossplots of Q and effective porosity (red diamonds in Figure 14) and total porosity (blue circles) were created for P- and shear wave respectively. It is clear that Q values of P-wave decrease with porosity. Q_s displays a similar variation, however the trend is not as strong as with Q_p . Perhaps Q_p is influenced more by fluids in the rock.

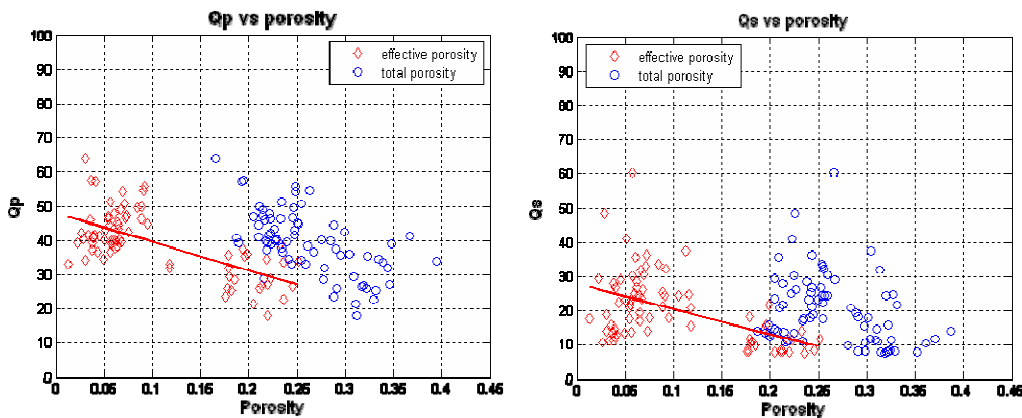


FIG. 14. Crossplot between Q_p and porosity (left: effective porosity in red; total porosity in blue) and Q_s vs. porosity (right).

Attenuation in shale and shaly sandstone

From the crossplot between Q value and shale volume (Figure 15), the maximum attenuation of the P wave was found in shaly sandstones in this well. The attenuation of the P wave was relatively small in clean sand and shale. However, it is generally believed that V_p/V_s increases with shale volume. This is not obvious in our current case. But, the S-sonic values may not be completely reliable. The Q vs. V_p/V_s relationship and the Q vs. shale volume relationship seem to be contradictory with this idea. Crossplots between

Vp/Vs and GR, and shale volume were created as shown in Figure 16. It indicates there is no apparent relationship between Vp/Vs and shale volume. Thus Q increase with shale volume is also possible. It does not contradict to the result that Q values decrease with increasing Vp/Vs.

According to the relationship between attenuation and fluid, it is possible that the interaction between mobile water in the pores and clay-bound water generates large attenuation of P wave. To investigate this idea, a crossplot between Q values and clay bound water were also created (Figure 17). Neutron porosity responds to the total water volume in the rock, which includes clay bound water and free water. Thus, the clay-bound water volume was estimated from the difference between neutron porosity and effective porosity and normalized by neutron porosity. When the water is 100% bound to clay, the attenuation will be small. While part of the water is free and the other is bound to clay, large attenuation will be generated. For the shear wave, a similar relation can also be observed. Since shear attenuation may be less related to pore fluid, the variations of Qs value with shale volume and clay bound water were not as distinct as Qp values.

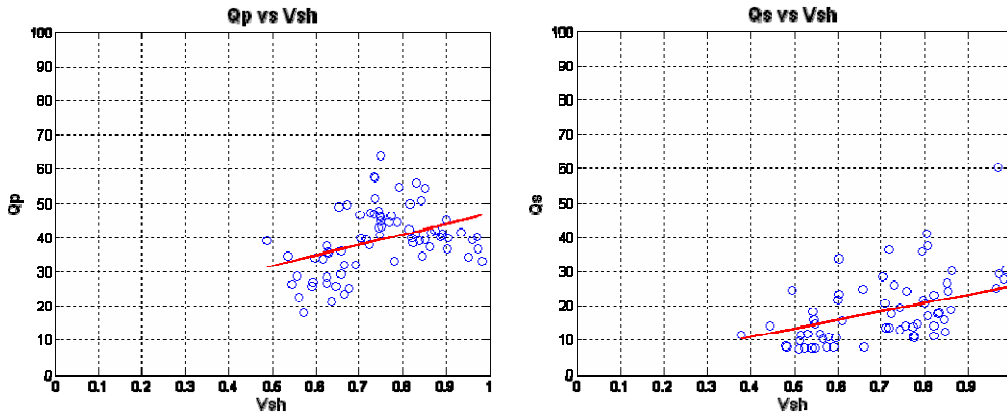


FIG. 15. Crossplot between Qp and shale volume (left), and Qs vs. shale volume (right).

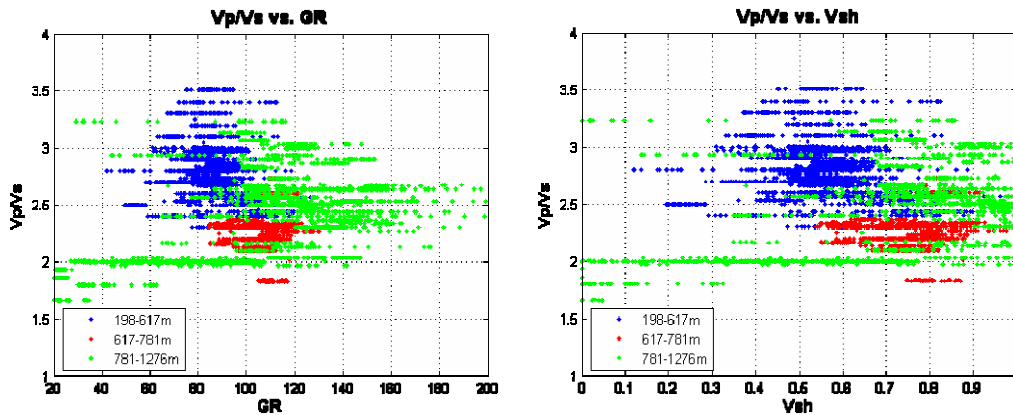


FIG. 16. Crossplot between Vp/Vs and GR (left), and VP/Vs vs. Vsh (right). Blue: 198-617m (above Milk River); red: 617-781m (Milk River-Colorado Group); green: 781-1276m (Colorado group and below).

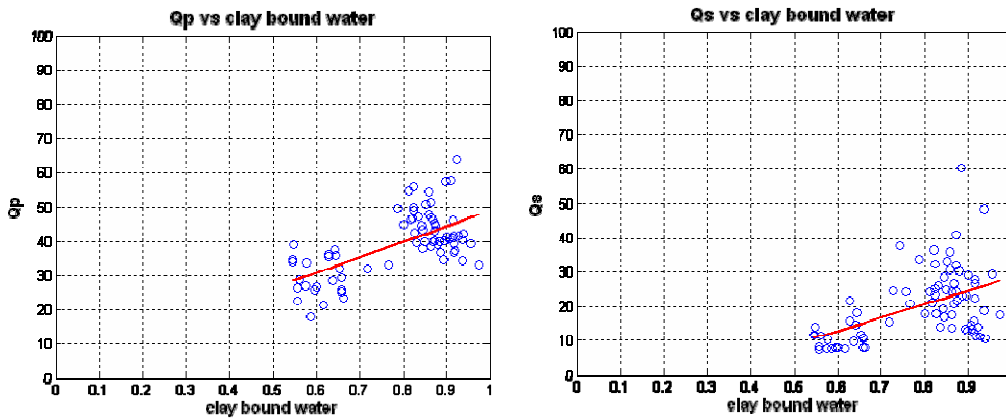


FIG. 17. Crossplot between Qp and clay bound water (left), and Qs vs. clay bound water (right).

Relationship between Qp and Qs

From the analysis of Q values and velocity, V_p/V_s , porosity, clay content and clay bound water, it appears that Qp and Qs display similar variation with these rock properties. The physical basis for the link of Qp and Qs is the fact that there is a shear element in compressional deformation. Mavko et al. (2005) derived relations between P-wave and S-wave attenuation based on Hudson's theory for a cracked medium,

$$\frac{Q_p^{-1}}{Q_s^{-1}} = \frac{1}{4} \frac{(M/G - 2)^2 (3M/G - 2)}{(M/G - 1)(M/G)} \quad (5)$$

Where M, G are P- and shear moduli respectively, and

$$\frac{M}{G} = \frac{2 - 2\nu}{1 - 2\nu} = \frac{V_p^2}{V_s^2} \quad (6)$$

Figure 18 displays Qp/Qs values from VSP data and Mavko's theoretical relation. For reliable estimated Q values for P- and shear wave over interval 400m-800m, the theoretical values present a nice correlation with field measurement. Figure 19 also displays the relationship between Qp and Qs. These two set of values have similar variation with depth.

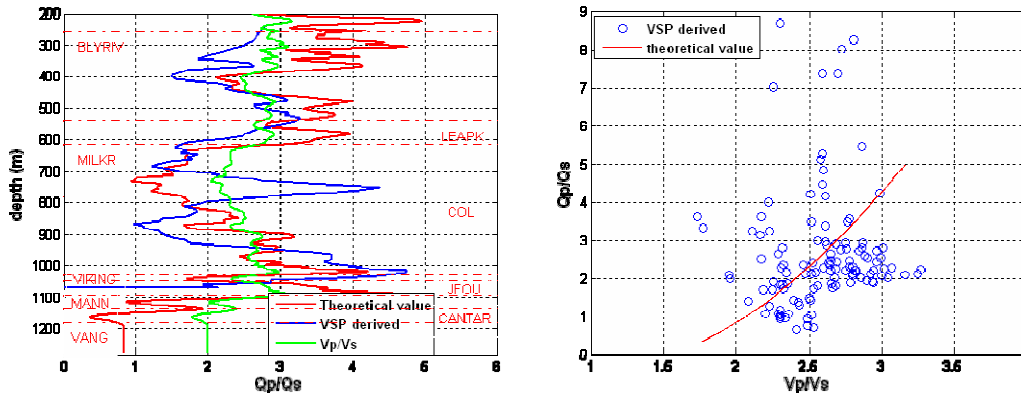


FIG. 18. Left, blue: Qp/Qs value from VSP data (smoothed using 3-point window); red: theoretical Qp/Qs value; green: Vp/Vs value from well log (Vp/Vs from well log data was smoothed using a 10m window). Right, crossplot between Qp/Qs and Vp/Vs, the red line is theoretical values.

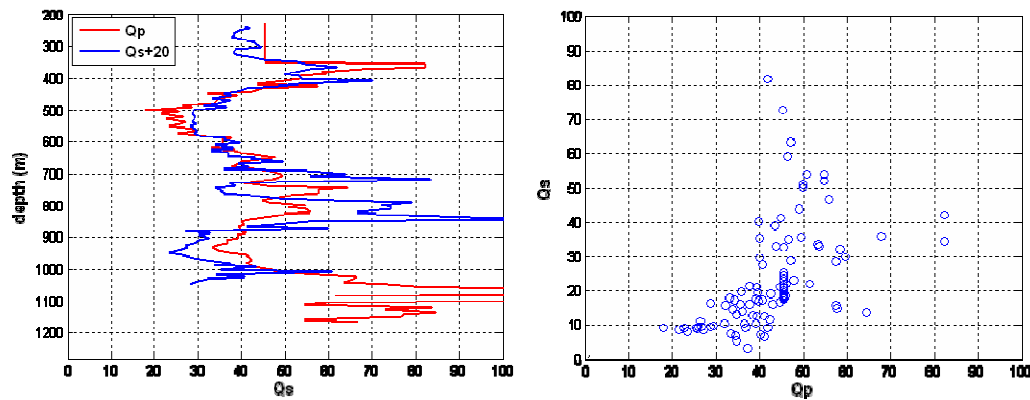


FIG. 19. Left, blue: Qp values; red: Qs+20. Right is the crossplot between Qp and Qs.

CONCLUSIONS

Well 11-25-13-17W3 from Ross Lake was selected for the analysis of relationship between seismic data attenuation and rock properties. Well log analysis indicates the studied depth interval is mainly shale and shaly sandstone. An interesting correlation between the Q values and rock properties was found over reliable Q estimation interval. Generally, increasing P- and S-velocities accompany a decreasing attenuation of P- and S-waves. Greater pore space in the rock and higher Vp/Vs coincide with low Qp and Qs values. Interestingly, attenuation was found to be increasing with clay content for high clay- content sandstone. Clean sand in this well shows less attenuation than shaly sandstone. The crossplot between Qp and clay bound water indicates more attenuation of shaly sandstone possibly caused by the interaction between mobile water and clay bound water.

Since attenuation of reservoir and wet sand in this well were not obtained in this study, the effect of different pore fluid on attenuation was not seen. If reliable attenuation can be acquired from surface seismic data, the rule of attenuation variation with different pore

fluid is possibly acquired. Thus, we might be able to use the attenuation characteristics of seismic data to differentiate hydrocarbons from water in the reservoir.

ACKNOWLEDGEMENTS

The authors would like to thank Husky Energy Inc. for providing the data. We appreciate GEDCO for donating VISTA software, and Rick Kuzmiski for instruction on VSP processing. Thanks also to the CREWES sponsors for their financial support.

REFERENCES

- Bale, R.A. and Stewart, R.R., 2002, The impact of attenuation on the resolution of multicomponent seismic data: CREWES Research Report, **14**.
- Haase, A. B., and Stewart, R. R., 2004, Attenuation Estimates from VSP and Log Data: 74th Ann. Internat. Mtg., SEG Exp. Abstr, 2497-2500.
- Hauge, P. S., 1981, Measurements of attenuation from vertical seismic profiles: *Geophysics* **46**, 1548-1558.
- Klimentos T., and McCann C., 1990, Relationships among compressional wave attenuation, porosity, clay content and permeability in sandstones: *Geophysics* **55**, 998-1014.
- Koesoemadinata, A. P., and McMechan, G. A., 2001, Empirical estimation of viscoelastic seismic parameters from petrophysical properties of sandstone: *Geophysics* **66**, 1457-1470.
- Mavko, G., and Dvorkin, J., 2005, A theoretical estimate of S-wave attenuation in sediment: 73rd Ann. Internat. Mtg., SEG Exp. Abstr, 1470-1474.
- Mukerji, T., and Mavko, G., 2006, Recent advances in rock physics and fluid substitution: CSEG Recorder 2006 Special Edition, 123-127.
- Toksöz, M. N., and Johnson, D. H., 1981, Seismic wave attenuation: Society of Exploration Geophysicists.
- Xu, C., and Stewart R.R, 2003, Ross Lake 3C-3D seismic survey and VSP, Saskatchewan: A preliminary interpretation, **15**: CREWES Research Report, 58:1-12.
- Xu, C., and Stewart R.R, 2005, Interval Q estimation and a quality indicator – QQI: CREWES Research Report, **05**:1-11.